Asia-Pacific Journal of
Chemical Engineering WILEY

Online estimation for catalyst activity of acetylene hydrogenation reactor

Fu-Ming Xie | Feng Xu | Zhi-Shan Liang | Xiong-Lin Luo

Department of Automation, China University of Petroleum, Beijing, China

Correspondence
Feng Xu, Department of Automation, China University of Petroleum, Beijing 102249, China.
Email: xufengfxzt@sohu.com

Funding information
National Natural Science Foundation of China, Grant/Award Number: 21676295

Abstract

In the ethylene industry, the high purity of the ethylene product depends on hydrogenation in acetylene hydrogenation reactor. Because the catalyst deactivation leads to the moving of the operating point, the operation scheme must be adjusted continually according to the catalyst activity. It is necessary to estimate the catalyst activity online. Based on the discrete dynamic model of the acetylene hydrogenation reactor, the extended Kalman filter (EKF) is used to build the soft sensor for catalyst activity. Considering that EKF involves the large computation costs, we propose a method that estimates the parameters of the time-varying deactivation kinetics model for the tradeoff of accuracy and complexity. The method is effective to reduce computation complexity of estimation, and simultaneously, the accuracy satisfies the process requirement.

KEYWORDS

acetylene hydrogenation reactor, catalyst activity deactivation, extended Kalman filter, soft sensor

1 | INTRODUCTION

The acetylene hydrogenation reactor is a common reactor for purifying ethylene stream in industry, where the palladium catalyst is often used.[1,2] For simplified modeling, the one-dimensional pseudo-homogeneous model has been widely accepted for the modeling of acetylene hydrogenation reactor.[3-5] Moreover, the improved bimetallic catalyst is also extensively utilized, and comprehensive research about modeling and analysis has been carried out.[6,7] For higher modeling accuracy, the two-dimensional heterogeneous model is also used for the modeling of acetylene hydrogenation reactor,[8,9] which is also of higher computation complexity. Based on these models, the relationship among variables is analyzed, and the nature of critical variables is elucidated.

During the running of acetylene hydrogenation reactor, the catalyst deactivation is an inevitable problem.[10,11] As the catalyst activity slowly declines with time, the operation must be adjusted. Modeling of catalyst deactivation has been studied by many scholars.[12-16] Several catalyst deactivation models are proposed, and the majority of studies consider that the catalyst deactivation is related to temperature and catalyst poisoning.[17,18] In practical production process, the fitted curve of industrial data is employed for temporary catalyst deactivation modeling, which is of no universality.

In industrial processes, it is necessary to obtain some key variables that cannot be measured through online estimation for better control and optimization,[19-21] so the method of soft sensor is developed. In recent years, the data-driven statistical regression soft sensor has been applied in chemical processes, such as principal component analysis,[22-24] partial least square,[25-27] artificial neural network,[28,29] support vector machine,[30,31] and just-in-time learning.[32-34] Considering the nonlinearities and time-varying characteristics, a soft sensor development based on supervised ensemble learning with

improved process state partition is proposed.[35] Deep learning, a subset of machine learning, is capable of learning deep, hierarchical artificial neural networks efficiently. In recent years, deep-learning-based architectures have been applied in data modeling of soft sensor.[36,37] Based on quality prediction and process monitoring methods in process industries, deep quality-related feature extraction with hybrid Variable-Wise weighted stack auto encoder (VW-SAE), hierarchical quality-relevant feature representation and extended deep belief network have been developed for soft sensing modeling.[38-40]

Although the model-driven soft sensor is more effective for specific plants, in the previous research of acetylene hydrogenation reactor, a simple soft sensor calibration scheme based on output correction is proposed.[41] In addition, dynamic modeling of soft sensor is a significant problem that should be addressed. In recent years, process data dynamic modeling approaches have been used for soft sensor, such as linear dynamic systems and long-short term memory.[42,43] For the state estimation problem for nonlinear systems, the extended Kalman filter (EKF) is employed, which is much favorable in practical process engineering.[44-46] In consideration of the errors resulting from linearization, a new robust design approach for a discrete-time EKF is proposed.[47] To handle the stochastic uncertainties in discrete-time nonlinear systems, a linearization error model is established as a norm-bounded uncertainty term for robust EKF.[48] It is provided that the continuous-discrete EKF is more accurate and preferable for practical use.[49-51]

In existing work, the catalyst activity of acetylene hydrogenation reactor is used as a lumped parameter or one-dimensional distribution parameter.[1-8] The activity of the catalyst after a long period of operation is calculated by the catalyst deactivation kinetic model, without considering the model mismatch caused by uncertain factors.[52] Thus, the main differences between this paper and the existing work are shown as follows: The catalyst activity is regarded as a two-dimensional distribution parameter for estimation and calculation; an online EKF estimator is constructed to estimate the activity accurately in real time, considering that estimated activity of distribution parameter consumes excessive computation time; and an improved EKF method based on the deactivation kinetic model of catalyst is proposed to reduce computation complexity and simultaneously to ensure estimation accuracy. Further, in this paper, Pareto set is used to analyze the discrete interval and the estimated parameters in the improved method, and the optimal strategy with satisfactory accuracy and estimated time is obtained.

2 | PROBLEM DESCRIPTION

Acetylene hydrogenation reactor is a device for removing acetylene from high concentration ethylene stream by catalytic hydrogenation. In the process of reaction, the catalyst activity in the reactor is gradually decreasing with time, until the reactor stops running and carries out catalytic regeneration. This process lasts for several months or even a year. The main products of the reaction are ethylene, ethane, and green oil. The content of acetylene in the reaction gas is small, and the content of acetylene at the reactor outlet needs to meet the process requirements. Generally, the reactor contains multiple beds, and a green oil cleaning device is set between the beds to remove the green oil carried in the gas after the reaction.

Catalyst deactivation is a complex process involving surface temperature variation of catalyst, accumulated oligomer by secondary reaction, and changes of molecular structure. For catalyst activity, a major factor is the temperature variation of the catalyst surface in the short run. But in the long run, surface micropores of catalyst are clogged with oligomer of secondary reaction, and it leads to the slow decreasing of catalyst activity. Instead of a lumped parameter or one-dimensional distribution parameter, this paper defines the catalyst activity as a two-dimensional distribution parameter of radical and axial direction $\theta(Z,R)$. Similarly, the oligomer concentration adhering to catalyst micropores by secondary reaction is also defined as a two-dimensional distribution parameter of radical and axial direction. As shown in Figure 1, the decreasing curves of catalyst activity in reactor axial have a different tendency.
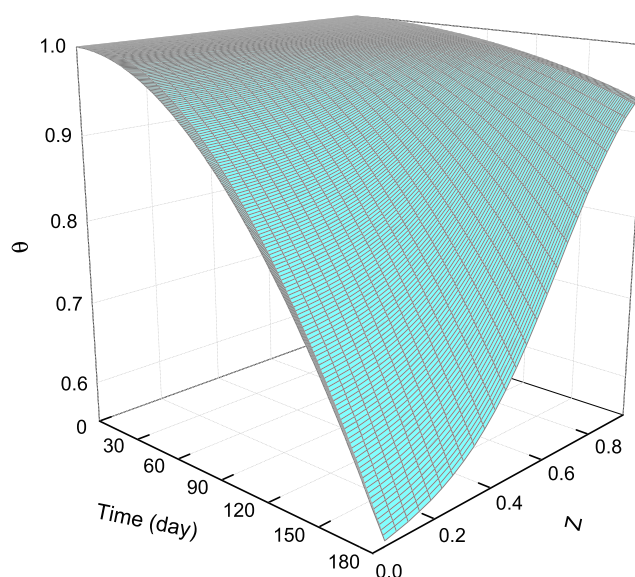

FIGURE 1 The catalyst activity of the first reactor bed at 180-day operation

The existing research of the acetylene hydrogenation reactor focus on offline operation optimization, but the optimal operating point will deviate because of decreasing catalyst activity with time. Compared with other disturbances, the decreasing catalyst activity has a significant effect on product. Thus, the two-dimensional heterogeneous deactivation model based on the intrinsic kinetics is used in this paper.

Figure 2 shows the tendency of optimal inlet temperature that is treated as one of commonly optimization variables in acetylene hydrogenation reactor. It illustrates that the optimal operation point of the actual reactor in the whole running cycle is related to the decreasing catalyst activity and the online catalyst activity estimation is necessary.

In our previous work, we realized the offline full cycle optimization of acetylene hydrogenation reactor,[52] taking the influence of catalyst deactivation into account. However, the offline optimization is difficult to cope with the activity changes caused by the unmeasurable uncertainties in actual industrial process. To make the feasible optimal operation strategy, the online soft sensor for catalyst activity is needed. The advantage of online soft sensor is that it could estimate real-time values of the state variables which are difficult to measure directly. By the online soft sensor of the acetylene hydrogenation reactor, the real-time activity of the catalyst could be obtained accurately, and the optimality and robustness of the operation and control strategy could be improved.

In addition, there are certain requirements for accuracy and estimation time of the online soft sensor. For the accuracy, the estimated mean standard deviation should not exceed the activity difference between the last day of the operating cycle and the day before, as shown in Table 1. Considering that the temperature runaway of the reactor caused by the sudden activity change must be
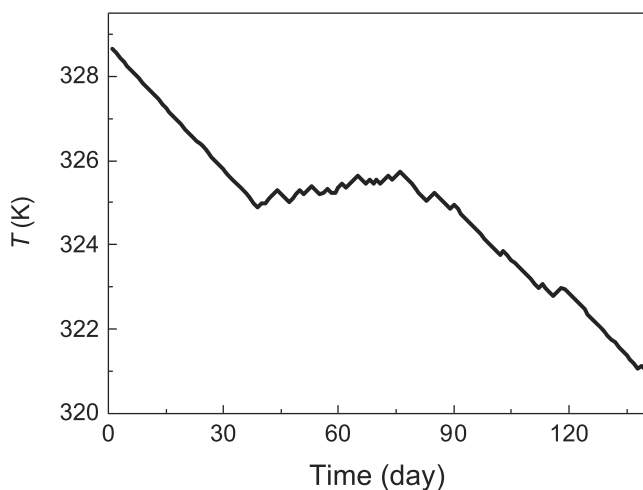
TABLE 1 Requirements of estimated accuracy and time[52]

Variable	Online optimization	Safe operation	APC
Catalyst activity deviation of inlet	≤0.014	≤0.014	≤0.010
Catalyst activity deviation of center	≤0.0064	≤0.0064	≤0.0059
Catalyst activity deviation of outlet	≤0.0018	≤0.0018	≤0.0018
Average activity deviation of the reactor	≤0.0076	≤0.0076	≤0.0063
The estimated time (s)	≤28,800	≤3,600	≤180

Abbreviation: APC, advance process controller.

avoided in the actual industrial process, the feedback of the activity in the reactor should be received regularly during operation. Hence, online calculation time of soft sensor should be controlled within 1 hr. In addition, if the reactor is controlled by an advanced process controller (APC), the online calculation time of soft sensor should be about 3 min.

3 | CATALYST ACTIVITY ESTIMATION OF EKF

In response to the above problem description, the two-dimensional heterogeneous model of the reactor is employed. In general, during operation optimization of the acetylene hydrogenation reactor, it is assumed that all the catalyst activity is equivalent in all internal sites of reactor. In this paper, considering the integrality of the acetylene hydrogenation reactor, the internal catalyst activity is treated as a two-dimensional distribution parameter. To design a soft sensor of activity, due to the long duration of the reactor (about a few months even 1 year), the model should be discretized. Considering the catalyst activity of radical and axial direction, the model has been established in our previous work.[52] Based on that, we propose the acetylene hydrogenation reactor model for discretization. $\theta(k)$ is defined as distribution catalyst activity of radical and axial direction. Mass balance discrete equation for fluid phase is as follows:

$$p_{ik}^g(Z,R,k) = p_{ik}^g(Z,R,k-1) + u(k)\frac{\partial p_{ik}^g(Z,R,k)}{\varepsilon\partial Z} + f_1(Z,R,k). \tag{1}$$

Thermal balance equation for fluid phase is as follows:

FIGURE 2 Optimal inlet temperature in a regenerate cycle

$$T_k^{\mathrm{g}}(Z,R,k) = T_k^{\mathrm{g}}(Z,R,k-1) - u(k)\frac{\partial T_k^{\mathrm{g}}(Z,R,k)}{\varepsilon \partial Z} + f_2(Z,R,k). \tag{2}$$

Mass balance equation for catalyst phase is as follows:

$$p_{ik}^{\mathrm{s}}(Z,R,k) = p_{ik}^{\mathrm{s}}(Z,R,k-1) + \frac{\theta(Z,R,k)\; r_i}{1-\varepsilon} + f_3(Z,R,k). \tag{3}$$

Thermal balance equation for catalyst phase is as follows:

$$T_k^{\mathrm{s}}(Z,R,k) = T_k^{\mathrm{s}}(Z,R,k-1) + \frac{\theta(Z,R,k)}{(1-\varepsilon)\rho_{\mathrm{s}}c_{\mathrm{ps}}}\sum_{j=1}^{2}\eta_j r_j \Delta H_j + f_4(Z,R,k), \tag{4}$$

where p is gas partial pressure in the reactor and T is temperature in the reactor. u is the control matrix; r is the reaction rate of the gas; ε is the porosity of catalyst; ρ is the average density; c_{p} is the heat capacity; and subscript i = a, b, and c is acetylene, ethylene, and hydrogen, respectively. Subscript k denotes the sequence number of reactor bed with k = 1, 2, and 3. Superscript s and g represent the variable of gaseous fluid phase and solid catalyst phase for the heterogeneous model. To simplify the equation, f_1–f_4 is the part that indirectly related to the estimated catalyst activity. Model parameters are shown in Table 2.

We want to estimate the internal activity of a three-stage acetylene hydrogenation reactor operating for 180 days. The inlet operating data of the three-stage bed reactor are shown in Table 3.

TABLE 2 Model parameters[52]

Variable	Model parameter	Value
ε	Catalyst porosity	0.35
η_1,η_2	Efficient factor of the ethylene and ethane generated reaction	3.461, 4.26 × 10^{-3}
c_{p}	Heat capacity(J·kg^{-1}·K^{-1})	1.724
E_{d}	Activation energy of catalyst deactivation (kJ·kmol^{-1})	9.9
$\Delta H_1,\Delta H_2$	Heat of the ethylene and ethane generated reaction (J·mol^{-1})	174.3,136.7
$k_{\mathrm{d}}, K_{\mathrm{d}}$	Catalyst deactivation coefficients	6.73 × 10^{-3}, 3.09 × 10^{-3}
R_{g}	Gas constant(J·mol^{-1}·K^{-1})	8.314

TABLE 3 Operational data for acetylene hydrogenation reactors

Operating variable	Value
$p_{\mathrm{c1}}^{\mathrm{g}}(0,R,k)$/kPa	29.55
$T_1^{\mathrm{g}}(0,R,k)$/K	320.80
$p_{\mathrm{a1}}^{\mathrm{g}}(0,R,k)$/kPa	29.55
$p_{\mathrm{b1}}^{\mathrm{g}}(0,R,k)$/kPa	1684.35
$p_{\mathrm{c2}}^{\mathrm{g}}(0,R,k)$/kPa	14
$T_2^{\mathrm{g}}(0,R,k)$/K	321.80
$p_{\mathrm{c3}}^{\mathrm{g}}(0,R,k)$/kPa	0.79
$T_3^{\mathrm{g}}(0,R,k)$/K	322.80
k/day	180

Kalman filter (KF) is the most widely used state estimation method that has been widely applied in communication, navigation, guidance and control, and other fields.[53] KF has many different forms. The most common application of the KF to nonlinear systems is in the form of EKF. Exploiting the assumption that all transformations are quasi-linear, the EKF simply linearizes all nonlinear transformations and substitutes Jacobian matrices for the linear transformations in the KF equations.[54] Considering that the acetylene hydrogenation reactor is a complex nonlinear system, EKF is adopted for online estimation of catalyst activity.

Based on acetylene hydrogenation reactor discrete model, catalyst activity discrete dynamic model is shown in Equations (5)–(7).

$$\theta(k) = H(k)\theta(k-1), \tag{5}$$

$$y(k) = h(\theta(k),u(k),v(k)), \tag{6}$$

$$v(k)^{\sim}(0,R_0), \tag{7}$$

where $\boldsymbol{h}$ is acetylene hydrogenation reactor discrete dynamic model, $\boldsymbol{v}$ is the associated measurement error that obeys normal distribution for catalyst activity, and $H(k)$ is linearization model based on catalyst deactivation kinetics equations, as shown in Equation (8).

$$H(k) = k_{\mathrm{d}}\left(\mathrm{e}^{-\frac{E_{\mathrm{d}}}{R_{\mathrm{g}}T^{\mathrm{s}}(k-1)}}\sum_{j=1}^{k-1}\frac{p_{\mathrm{a}}^{\mathrm{s}\,2}(j)p_{\mathrm{c}}^{\mathrm{s}}(j)}{\left(1+K_{\mathrm{d}}p_{\mathrm{a}}^{\mathrm{s}}(j)\right)^3} - \mathrm{e}^{-\frac{E_{\mathrm{d}}}{R_{\mathrm{g}}T^{\mathrm{s}}(k)}}\sum_{j=1}^{k}\frac{p_{\mathrm{a}}^{\mathrm{s}\,2}(j)p_{\mathrm{c}}^{\mathrm{s}}(j)}{\left(1+K_{\mathrm{d}}p_{\mathrm{a}}^{\mathrm{s}}(j)\right)^3}\right) \tag{8}$$

Estimation error covariance of the catalyst activity $\theta(k)$ is defined as $P(k) = E\left\{\left[\theta(k)-\hat{\theta}(k)\right]\left[\theta(k)-\hat{\theta}(k)\right]^{\mathrm{T}}\right\}$. Prior estimation and posteriori estimation of $\theta(k)$ is

respectively defined as $\hat{\theta}^-(k)$ and $\hat{\theta}^+(k)$. EKF equations for $\theta(k)$ is shown in Equations (9)–(14):

$$\hat{\theta}^-(k) = H(k)\hat{\theta}^+(k-1), \tag{9}$$

$$P^-(k) = H(k)P^+(k-1)H(k)^{\mathrm{T}}. \tag{10}$$

Equations (9)–(10) are respectively update equations of the catalyst activity and the estimation error covariances from k-1 to k. The Jacobian matrices of partial derivative of $\boldsymbol{h}$ with respect to catalyst activity and the associated measurement error are respectively represented as $\boldsymbol{Q}$ and $\boldsymbol{M}$.

$$Q(k) = \frac{\partial h}{\partial \theta}\Big|_{\hat{\theta}^-(k)}, M(k) = \frac{\partial h}{\partial v}\Big|_{\hat{\theta}^-(k)} \tag{11}$$

$\boldsymbol{K}$ is the Kalman gain, which is derived as follows:

$$K(k) = P^-(k)Q^{\mathrm{T}}(k)\left[Q(k)P^-(k)Q^{\mathrm{T}}(k) + M(k)R_0 M^{\mathrm{T}}(k)\right] \tag{12}$$

Combing the prior estimate, it is feasible to obtain an update equation for the estimate of the catalyst activity:

$$\hat{\theta}^+(k) = \hat{\theta}^-(k) + K(k)\left\{y(k) - h\left[\hat{\theta}^-(k), u(k), 0\right]\right\} \tag{13}$$

The error covariance update equation is derived as follows:

$$P^+(k)K(k) = [I - K(k)Q(k)]P^-(k)[I - K(k)Q(k)]^{\mathrm{T}} + K(k)M(k)R_0 K^{\mathrm{T}}(k)M^{\mathrm{T}}(k) \tag{14}$$

Based on EKF equations, the online estimation of catalyst activity $\hat{\theta}(k)$ can be implemented. However, in view of high calculation complexity of large scale matrix iteration in $\theta(k)$ estimated, the activity of the reactor inlet and outlet $\theta(0,R,k)$ and $\theta(1,R,k)$ replace $\theta(k)$ as the estimated catalyst activity matrix and are used to calculate all discrete points in the reactor based on two-dimensional heterogeneous discrete model. $H(k)$ is obtained by linearization model of acetylene hydrogenation reactor. As a consequence of the aforementioned analysis, the specific soft sensor structure based on EKF is shown in Figure 3. The plant model of literature 52 including mechanism model of the acetylene hydrogenation reactor and the control system is used for testing the estimator.

Considering that the activity of the reactor inlet and outlet is unable to update state variables and Jacobian matrices, the prior estimates $\hat{\theta}^-(0,R,k)$ and $\hat{\theta}^-(1,R,k)$ are substituted into the two-dimensional heterogeneous discrete model and the prior estimate of the activity of the whole reactor $\hat{\theta}^-(k)$ is obtained. Then, the activity of the whole reactor is used for update equation of the catalyst activity (Eq.(9)) and obtaining the Jacobian matrices (Equation (11)). The estimation error covariance and Kalman gain are updated by state variables and Jacobian matrices of the reactor inlet and outlet. Thus, the prior activity estimates of the reactor inlet and outlet are updated. Because primary update equations of EKF are simplified, the catalyst activity of the whole reactor is shortly estimated.

Generally, the acetylene hydrogenation reactor contains two to three fixed beds. However, the first bed suffers the fastest catalyst activity decreasing and absorbs over 95% of total acetylene, simultaneously the catalyst activity decreasing in the second and third bed is imperceptible and unworthy to be estimated. Hence, this paper only provides online activity estimation on the first bed to reduce the computation burden. As shown in Figure 4, the catalyst activity of the reactor inlet is accurately tracked by EKF with error less than $\pm 1 \times 10^{-2}$. Compared with estimation of the reactor inlet, as shown in Figure 4, the estimated value of the reactor center is of relative larger deviation to the actual value because it is obtained by two-dimensional heterogeneous model. Considering that the catalyst activity decreasing of the reactor outlet is slow and slight, as shown in Figure 4, its tendency of the estimated value is not obvious, but the actual deviation is minuscule and the effect could be ignored. The EKF based soft sensor is efficient on tracking for catalyst activity decreasing trajectory and the estimation accuracy meets the requirements in Table 1. However, considering that the computation time is consumed more than 1 hr, as shown in Table 4, it does not meet the requirement of safe operation.

4 | IMPROVED EKF ACTIVITY ESTIMATION METHOD BASED ON DEACTIVATION EQUATION

Although the EKF based soft sensor could give accurate estimated value of catalyst activity, the large scale estimated catalyst activity matrix still leads to more calculation complexity and more calculation time. The purpose of the paper is to figure out a fast and efficient estimation method that can satisfy the requirements of accuracy and computation complexity. Thus, we propose an improved EKF-based soft sensor according to the variable parameter model of catalyst deactivation. Considering that the deactivation kinetic equation is generally appropriate for
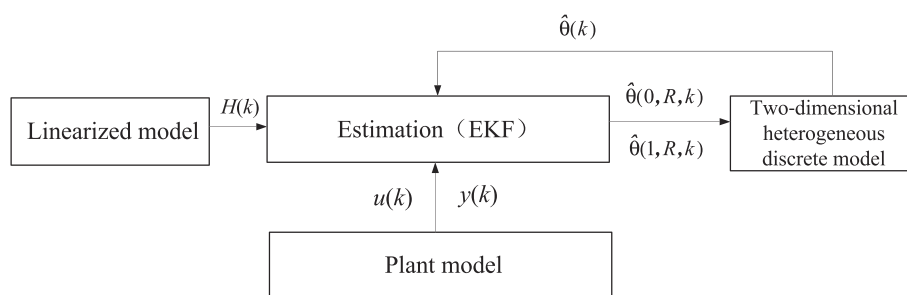
FIGURE 3 Catalyst activity estimator structure. EKF, extended Kalman filter
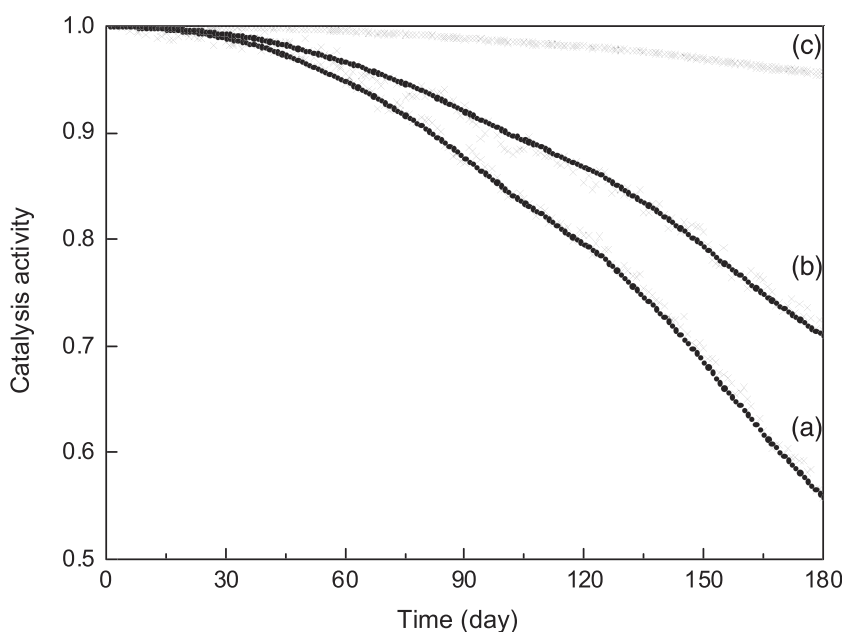
FIGURE 4 Catalyst activity estimation by extended Kalman filter at 180-day operation. "a" indicates catalyst activity estimation of reactor inlet; "b" indicates catalyst activity estimation of reactor center; "c" indicates catalyst activity estimation of reactor outlet; dots "·" indicate catalyst activity; and symbol "×" indicates estimation of catalyst activity

TABLE 4 Comparing with EKF and improved method

Variable	EKF	Improved
Estimation standard deviation of inlet	0.006213	0.006279
Estimation standard deviation of center	0.007605	0.003036
Estimation standard deviation of outlet	0.000873	0.001216
Time running on the CPU (s)	3,874	436

Abbreviations: CPU, central processing unit; EKF, extended Kalman filter.

acetylene hydrogenation reactor, the improved EKF based soft sensor could accurately track the trajectory of catalyst activity.

Catalyst deactivation equation obtains three variable parameters: deactivation coefficient k_d and K_d and deactivation energy E_d. For convenience, we define $\lambda = [\lambda_1, \lambda_2, \lambda_3]$ as estimated target matrix. Then the time-varying deactivation equation and discrete dynamic model are built, as shown in Equations (15)–(18). Equation (15) is the conversion equation of catalyst activity and deactivation parameters, and the linear model $H_1(k_1)$ can be obtained by combining Equations (15), (5), and (16). $N(k)$ and $N(k_1)$ represent the number of k and k_1, respectively. In addition, to reduce computation complexity, the discrete interval of improved method could be several times of the previous interval, where the discrete variable is represented by k_1.

$$\theta(\lambda(k_1),k)=\theta(\lambda(k_1),k-1)-\lambda_1(k_1)e^{-\frac{\lambda_2(k_1)}{R_g T^s(k)}}\sum_{j=1}^{k}\frac{p_a^{s\,2}(j)p_c^s(j)}{\left(1+\lambda_3(k_1)p_a^s(j)\right)^3}$$

(15)

$$\lambda(k_1)=H_1(k_1)\lambda(k_1-1)$$

(16)

$$y_1(k)=h_1(\lambda(k_1),u(k),v_1(k))$$

(17)

$$v_1(k)(0,\tilde{R}_1)$$

(18)

$$N(k)=nN(k_1) \quad n\in N^+$$

(19)

Equations (15)–(17) are substituted into Equations (9)–(14), and the corresponding EKF equations

are established. The estimated error covariance of the catalyst deactivation parameters $\lambda(k_1)$ is defined as $P(k_1) = E\left\{[\lambda(k_1) - \hat{\lambda}(k_1)][\lambda(k_1) - \hat{\lambda}(k_1)]^{\mathrm{T}}\right\}$. Prior estimation and posteriori estimation of $\lambda(k_1)$ are respectively defined as $\hat{\lambda}^+(k_1)$ and $\hat{\lambda}^-(k_1)$. Estimation equations of EKF for $\lambda(k_1)$ are shown in Equations (20)–(25):

$$\hat{\lambda}^-(k_1) = H_1(k_1)\hat{\lambda}^+(k_1 - 1), \tag{20}$$

$$P^-(k_1) = H_1(k_1)P^+(k_1 - 1)H(k_1)^{\mathrm{T}}. \tag{21}$$

The Jacobian matrices of partial derivative of $\boldsymbol{h_1}$ with respect to the catalyst deactivation parameters and the associated measurement error are respectively represented as $\boldsymbol{Q}$ and $\boldsymbol{M}$.

$$Q(k_1) = \left.\frac{\partial h_1}{\partial \lambda}\right|_{\hat{\lambda}^-(k_1)}, M(k_1) = \left.\frac{\partial h_1}{\partial v_1}\right|_{\hat{\lambda}^-(k_1)} \tag{22}$$

$\boldsymbol{K}$ is derived as follows:

$$K(k_1) = P^-(k_1)Q^{\mathrm{T}}(k_1)\left[Q(k_1)P^-(k_1)Q^{\mathrm{T}}(k_1) + M(k_1)R_1M^{\mathrm{T}}(k_1)\right]. \tag{23}$$

Combing the prior estimate, it is feasible to obtain an update equation for the estimate of the catalyst deactivation parameters:

$$\hat{\lambda}^+(k_1) = \hat{\lambda}^-(k_1) + K(k_1)\left\{y(k_1) - h_1\left[\hat{\lambda}^-(k_1), u(k), 0\right]\right\}. \tag{24}$$

The error covariance update equation is derived as follows:

$$P^+(k_1)K(k_1) = [I - K(k_1)Q(k_1)]P^-(k_1)[I - K(k_1)Q(k_1)]^{\mathrm{T}} + K(k_1)M(k_1)R_1K^{\mathrm{T}}(k_1)M^{\mathrm{T}}(k_1). \tag{25}$$

In addition, considering that measurement matrix $y_1(k)$ and control matrix $u(k)$ are mismatching to the estimated catalyst activity matrix $\hat{\lambda}(k_1)$, $y_1(nk_1)$, and $u(nk_1)$

are treated as the measurement matrix and control matrix instead of $y_1(k)$ and $u(k)$. The improved soft sensor structure is shown in Figure 5. $\hat{\lambda}(k_1)$ is obtained using EKF and substituted into catalyst deactivation model for obtained online activity estimation $\theta(k)$.

Based on above structure and equations, the improved soft sensor is implemented at 180-day operation. As shown in Figure 6, compared with Figure 4, the estimated standard deviations of the reactor inlet are slightly higher. However, the estimated standard deviations of the reactor center and outlet are slightly lower than the previous estimation result.

On the whole, there is not much difference between the two methods in view of the estimation error. However, for computation complexity, according to the performance comparisons in Table 4, the time consumption of the improved method is much less than previous estimation. The estimated time of the improved EKF meets the requirements of safe operation of the acetylene hydrogenation reactor. However, the estimated time should be further shortened when applied to the reactor with APC. The running environment of the soft sensor is Intel Core i7-8750H CPU.

In addition, the discrete interval and number of estimation parameters influence the performance of activity estimation. According to the performance comparisons in Table 4, under the condition of $\lambda = [\lambda_1, \lambda_2, \lambda_3]$, the discrete interval increasing leads the estimated time decreasing but the estimated standard deviations increasing. To the contrary, under the condition of $N(k) = 7N(k_1)$, the number decreasing of estimation parameters leads to the estimated time decreasing but the estimated standard deviations increasing. According to estimation performance in Table 5, the estimated standard deviations of $n = 2$ and 7 have deviation much less than $n = 7$ and 12, in consideration of estimated time, $n = 7$ should be appropriate. However, the estimated standard deviations of $\lambda = [\lambda_1]$ and $\lambda = [\lambda_1, \lambda_2]$ have large deviation compared with $\lambda = [\lambda_1, \lambda_2, \lambda_3]$. Thus, the deactivation parameters are indispensable for the soft sensor.

Although a good result is obtained in Table 5, the above analysis is considered poor sample number and unpersuasive discussion. For further researching of optimal option within different discrete intervals, the Pareto set is gained by average standard deviation of the
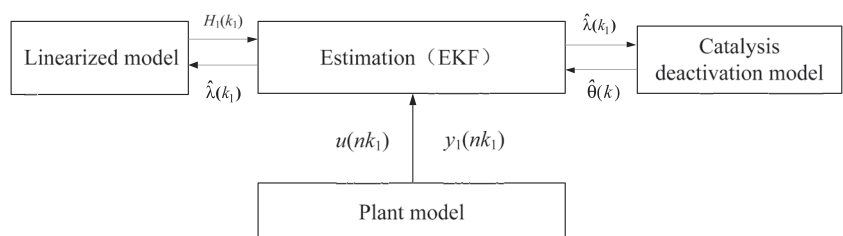

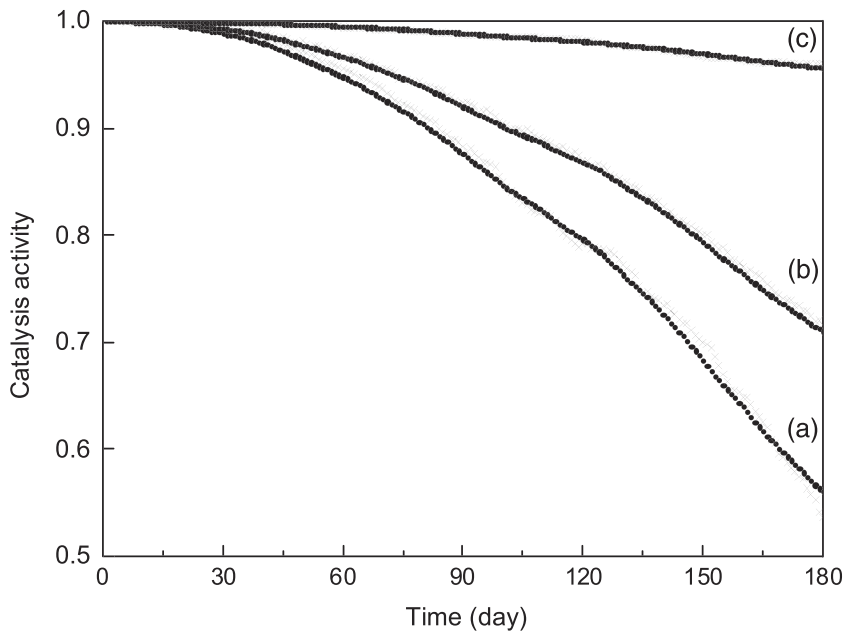**FIGURE 5** The improved soft sensor for activity. EKF, extended Kalman filter

FIGURE 6 Improved online activity estimation method at 180-day operation. "a" indicates catalyst activity estimation of reactor inlet; "b" indicates catalyst activity estimation of reactor center; "c" indicates catalyst activity estimation of reactor outlet; dots "·" indicate catalyst activity; and symbol "×" indicates estimation of catalyst activity

TABLE 5 Performance comparisons among different discrete intervals and number of estimation parameters

Variable	Discrete interval			Estimation parameter		
	$N(k) = 2N(k_1)$	$N(k) = 7N(k_1)$	$N(k) = 12N(k_1)$	λ_1	λ_1, λ_2	$\lambda_1, \lambda_2, \lambda_3$
Estimation standard deviation of inlet	0.006017	0.006279	0.007146	0.015901	0.009058	0.006279
Estimation standard deviation of center	0.002953	0.003036	0.003321	0.009562	0.005341	0.003036
Estimation standard deviation of outlet	0.000970	0.001216	0.001839	0.006533	0.002451	0.001216
Time running on the CPU (s)	879	436	217	93	208	436

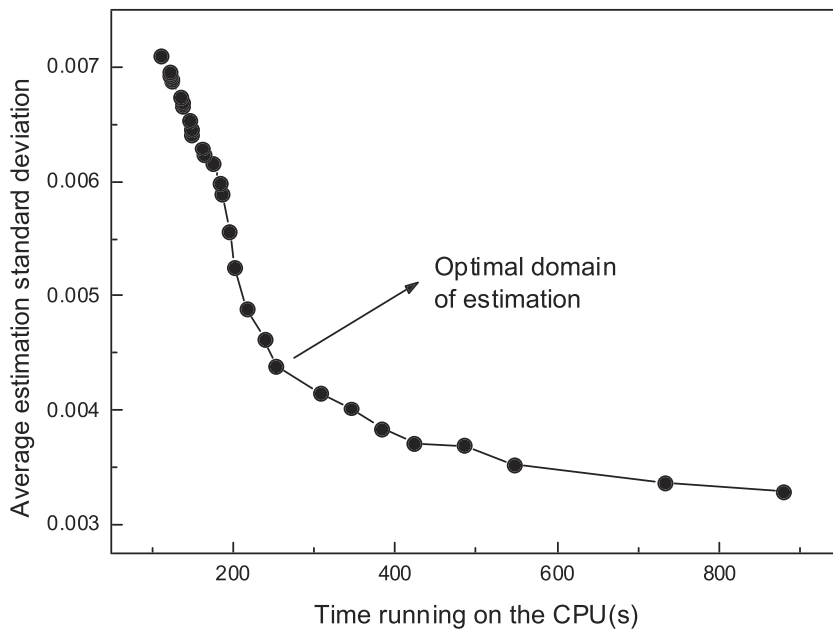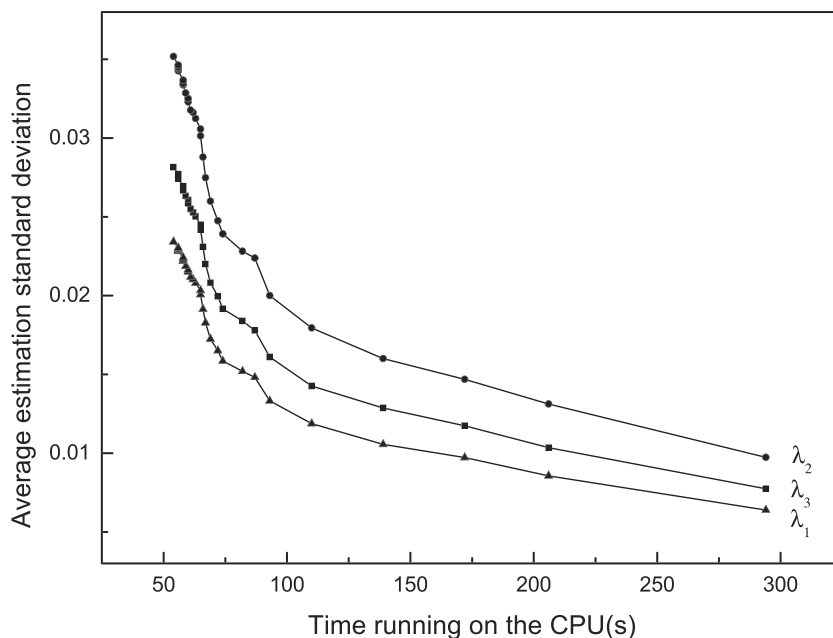Abbreviation: CPU, central processing unit.

FIGURE 7 Pareto curve of the different discrete estimation intervals with $\lambda = [\lambda_1, \lambda_2, \lambda_3]$. CPU, central processing unit

estimation in the whole reactor with estimation parameters $\lambda = [\lambda_1, \lambda_2, \lambda_3]$. Different discrete intervals of 29 integers are fetched in $n = [2,30]$. The Pareto curve is shown in Figure 7.
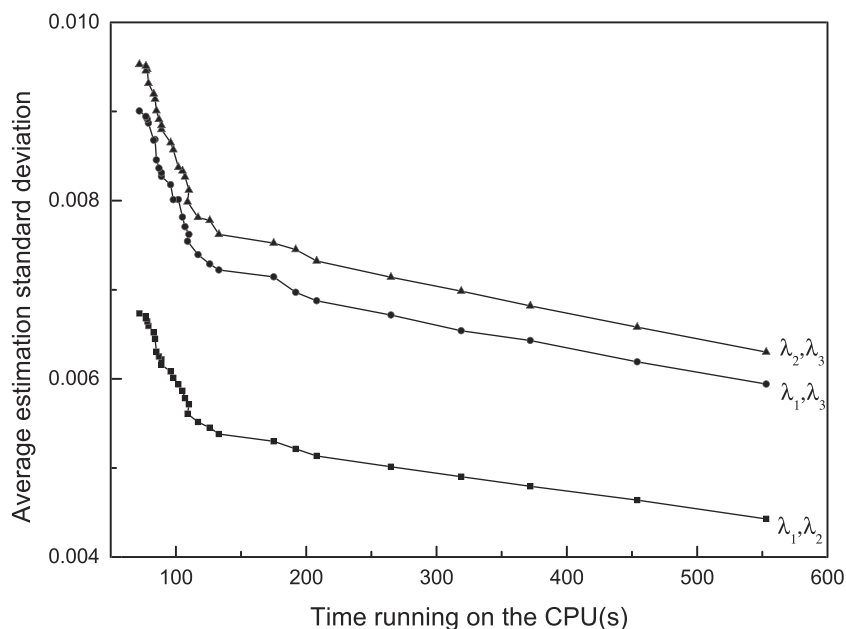
As shown in Figure 7, considering the estimation time and average estimated standard deviation, the point of $n = 9$ is the optimal point derived. Further, for the estimated time and standard deviation, the effect of the estimated parameters is discussed by the Pareto sets with combinations of λ. The Pareto curve that is gained with $\lambda = [\lambda_1],[\lambda_2],[\lambda_3]$ estimation is shown in Figure 8.

As shown in Figure 8, although the estimated time of $\lambda = [\lambda_1],[\lambda_2],[\lambda_3]$ is far less than $\lambda = [\lambda_1, \lambda_2, \lambda_3]$, it has more deviation on the catalyst activity estimation. In Figure 8, for estimation with $\lambda = [\lambda_1]$, the point of $n = 7$ is the optimal point derived by considering the estimated time and average estimated standard deviation. For estimation with $\lambda = [\lambda_2],[\lambda_3]$, the optimal point is respectively considered the point of $n = 6$ and $n = 5$. In addition, for the improved method that catalyst activity is estimated by one of the estimation parameters, influence of estimated parameters is in order of $\lambda_1 > \lambda_2 > \lambda_3$ on average estimated standard deviation. It is also indicative

FIGURE 8 Pareto curve of the different discrete estimation intervals with $\lambda = [\lambda_1],[\lambda_2],[\lambda_3]$. CPU, central processing unit

FIGURE 9 Pareto curve of the different discrete estimation intervals with $\lambda = [\lambda_1, \lambda_2], [\lambda_2, \lambda_3],[\lambda_1, \lambda_3]$. CPU, central processing unit

of the relative importance degree of the deactivation coefficient k_d, K_d, and deactivation energy E_d for catalyst deactivation.

Moreover, considering that the above two schemes are difficult to meet APC on estimation error or time, the tradeoff of estimation schemes is proposed. Similarly, to discuss the improved method of two estimation parameters, Pareto curve of $\lambda = [\lambda_1, \lambda_2], [\lambda_2, \lambda_3], [\lambda_1, \lambda_3]$ is gained and shown in Figure 9.

As shown in Figure 9, for estimation with $\lambda = [\lambda_1, \lambda_2]$, the point of $n = 9$ is the optimal point derived by considering the estimated time and average estimated standard deviation. But for estimation with $\lambda = [\lambda_2, \lambda_3]$ and $\lambda = [\lambda_1, \lambda_3]$, the point of $n = 6$ and $n = 7$ is the optimal point. In consideration of that estimation with $\lambda = [\lambda_1, \lambda_2]$ is better than $\lambda = [\lambda_2, \lambda_3]$ or $\lambda = [\lambda_1, \lambda_3]$ on average estimated standard deviation and the estimated time difference is not significant, it is considered for optimal option to estimate catalyst online. The scheme can meet the requirements of safe operation and advanced control in terms of estimated time and accuracy.

5 | CONCLUSIONS

For optimal operation with the reactor running for a long time, the paper establishes the EKF-based soft sensor for tracking tendency of the catalyst activity that is the dominant factor of operation point deviation. Although the estimated error of the EKF is available, it is difficult to be applied in practice because of its high computation complexity. Hence, the paper proposes an improved EKF estimator for more efficient estimation. The improved method builds variable parameter estimator based on catalyst deactivation model, efficiently reducing computation complexity simultaneously ensuring minor estimated error. In addition, considering that estimation performance and estimated time are affected by discrete interval and number of estimation parameters, the paper discusses the optimal option for balance of accuracy and computational complexity. Furthermore, the Pareto set is constructed by multiple estimation taking different parameter estimation combinations and estimated time intervals, so as to find the optimal estimation scheme that comprehensively considers the average estimated standard deviation and estimated time.

The improved EKF method could also be applied to most of the estimation of some parameters that cannot be directly measured and substantially changes the system, such as the heat transfer coefficient of the heat exchangers and the catalyst activity of various fixed-bed reactors. If these parameters are accurately and real-time estimated, it contributes to more optimal operational strategies and achieves better control and optimization effects. Considering that the improved EKF method relies on accurate mathematical models, the estimation accuracy of the method will be greatly reduced if structure changes of the model and substantial model mismatches occur. It can be considered to add the data-driven statistical regression soft sensor to verify EKF estimation results, such as principal component analysis, support vector machine and even deep learning. Timely verification could improve the robustness of the online soft sensor.

NOMENCLATURE

c_p	heat capacity(J·kg^{-1}·K^{-1})
E_d	activation energy of catalyst deactivation (kJ·kmol^{-1})
H, H_1	linearization model based on catalyst deactivation kinetics equations of EKF and improved EKF
h, h_1	acetylene hydrogenation reactor discrete dynamic model of EKF and improved EKF
$\Delta H_1, \Delta H_2$	heat of the ethylene and ethane generated reaction (J·mol^{-1})
K	Kalman gain
k, k_1	discrete variable of EKF and improved EKF
k_d, K_d	catalyst deactivation coefficients
M	The Jacobian matrices of partial derivative of h with respect to the associated measurement error
N	the number of discrete variables
P	estimation error covariance of the catalyst activity
p_a, p_b, p_c	acetylene, ethylene, and hydrogen pressure in the reactor (kPa)
p^s, p^g	the catalyst and the gas phase average gas pressure in the reactor (kPa)
p_{i1}, p_{i2}, p_{i3}	gas pressure in the 1-3 stage reactor (kPa)
Q	The Jacobian matrices of partial derivative of h with respect to catalyst activity or variable parameters
R	dimensionless radius of the reactor
R_0, R_1	covariance matrix of the associated measurement error of EKF and improved EKF
R_g	gas constant(J·mol^{-1}·K^{-1})
r_a, r_b, r_c	reaction rate of acetylene, ethylene, and hydrogen in the reactor (mol·m^{-3}·s^{-1})
r_g	reaction rate of green oil in the reactor (mol·m^{-3}·s^{-1})
r_1, r_2, r_3	reaction rate in the 1–3 stage reactor (mol·m^{-3}·s^{-1})
T^s, T^g	the catalyst phase and the gas phase temperature in the reactor (K)

T_1, T_2,
T_3 temperature in the 1–3 stage reactor (K)

u operation variable

v, v_1 the associated measurement error of EKF and improved EKF

y output of the catalyst activity discrete dynamic model

Z dimensionless axial of the reactor

ε catalyst porosity

η_1, η_2 efficient factor of the ethylene and ethane generated reaction

θ catalyst activity

ρ average density (kg·m^{-3})

λ_1, λ_2, λ_3 variable parameters: deactivation coefficient k_d and K_d, deactivation energy E_d

ORCID

Fu-Ming Xie https://orcid.org/0000-0002-5050-8756
Feng Xu https://orcid.org/0000-0003-0065-8016
Zhi-Shan Liang https://orcid.org/0000-0002-1295-0420
Xiong-Lin Luo https://orcid.org/0000-0002-3677-3182

REFERENCES

1. García-Mota M, Bridier B, Pérez-Ramírez J, López N. Interplay between carbon monoxide, hydrides, and carbides in selective alkyne. *J Catal.* 2010;273(2):92-102.
2. Molnár A, Sárkány A, Varga M. ChemInform Abstract: hydrogenation of carbon—carbon multiple bonds: chemo-, regio- and stereo-selectivity. *J Mol Catal A Chem.* 2001;173(1-2):185-221.
3. Tu F, Qing HY, Luo XL, et al. Advanced process control of acetylene hydrogenation reactor (I): construct dynamic model. *Control Instrum Chem Ind.* 2003;30(1):20-24.
4. Weiss G. Modeling and control of the acetylene converter. *J Process Control.* 1996;6(1):7-15.
5. Gobbo R, Soares RP, Lansarin MA, Secchi AR, Ferreira JMP. Modeling, simulation, and optimization of a front-end system for acetylene hydrogenation reactors. *Braz J Chem Eng.* 2004;21(4):545-556.
6. Huang W, Mccormick JR, Lobo RF, Chen J. Selective hydrogenation of acetylene in the presence of ethylene on zeolite-supported bimetallic catalysts. *J Catal.* 2007;246(1):40-51.
7. Pachulski A, Schodel R, Claus P. Kinetics and reactor modeling of a Pd-Ag/Al$_2$O$_3$ catalyst during selective hydrogenation of ethyne. *Appl Catal A:Gen.* 2012;445-446(6):107-120.
8. Szukiewicz M, Kaczmarski K, Petrus R. Modeling of fixed-bed reactor: two models of industrial reactor for selective hydrogenation of acetylene. *Chem Eng Sci.* 1998;53(1):149-155.
9. Luo XL, Liu JX, Xu F, et al. Hydrogenation, two-dimensional dynamic modeling and analysis of acetylene hydrogenation reactor. *CIESC J.* 2008;59(6):1454-1461.
10. Tian L, Jiang D, Qian F. Reactor system switch strategy for acetylene hydrogenation process. *CIESC J.* 2015;66(1):373-377.
11. Tian L, Jiang D, Qian F. Simulation and optimization of acetylene converter with decreasing catalyst activity. *CIESC J.* 2012;63(1):185-192.
12. Ravanchi MT, Sahebdelfar S. Pd-Ag/Al$_2$O$_3$ catalyst: stages of deactivation in tail-end acetylene selective hydrogenation. *Appl Catal A:Gen.* 2016;525:197-203.
13. Kuhn M, Lucas M, Claus P. Precise recognition of catalyst deactivation during acetylene hydrogenation studied with the advanced TEMKIN reactor. *Cat Com.* 2015;72(2):170-173.
14. Mccue AJ, Mcritchie CJ, Shepherd AM, et al. Cu/Al$_2$O$_3$ catalysts modified with Pd for selective acetylene hydrogenation. *J Catal.* 2014;319:127-135.
15. Albers P, PietschI J, Parker SF. Poisoning and deactivation of palladium catalysts. *J Mol Catal A Chem.* 2001;173(1):275-286.
16. Rahimpour MR, Dehghani O, Gholipour MR, et al. A novel configuration for Pd/Ag/a-Al$_2$O$_3$ catalyst regeneration in the acetylene hydrogenation reactor of a multi feed cracker. *Chem Eng J.* 2012;198-199:491-502.
17. Borodzinski A, Cybulski A. The kinetic model of hydrogenation of acetylene–ethylene mixtures over palladium surface covered by carbonaceous deposits. *Appl Catal A:Gen.* 2000;198(1):51-66.
18. Brown MW, Penlidis A, Sullivan GR. Control policies for an industrial acetylene hydrogenation reactor. *Can J Chem Eng.* 2010;69(1):56-59.
19. Joseph B, Brosilow C. Inferential control of processes Part I: steady state analysis and design. *AIChE J.* 1978;24(3):485-492.
20. Brosilow C, Tong M. Inferential control of processes Part II: the structure and dynamics of inferential control systems. *AIChE J.* 1978;24(3):492-500.
21. Joseph B, Brosilow C. Inferential control of processes Part III: construction of optimal and suboptimal dynamic estimators. *AIChE J.* 1978;24(2):500-509.
22. Ge ZQ, Song ZH. Semisupervised Bayesian method for soft sensor modeling with unlabeled data samples. *AIChE J.* 2011;57(8):2109-2118.
23. Zhao Y. A soft sensor based on orthogonal nonlinear principal component analysis. *Asia-Pac J Chem Eng.* 2008;13(3-4):233-242.
24. Zhu J, Gen Z, Song Z. Robust supervised probabilistic principal component analysis model for soft sensing of key process variables. *Chem Eng Sci.* 2015;122(27):573-584.
25. Galicia HJ, He QP, Wang J. A reduced order soft sensor approach and its application to continuous digester. *J Pro Contr.* 2011;21(4):489-500.
26. Yu J. Multiway Gaussian mixture model based adaptive kernel partial least squares regression method for soft sensor estimation and reliable quality prediction of nonlinear multiphase batch processes. *Ind Eng Chem Res.* 2012;51(40):13227-13237.
27. Shao W, Tian X, Wang P, Deng X, Chen S. Online soft sensor design using local partial least squares models with adaptive process state partition. *Chemometr Intell Lab.* 2015;144(15):108-121.
28. Himmelblau DM. Accounts of experiences in the application of artificial neural networks in chemical engineering. *Ind Eng Chem Res.* 2008;47(16):5782-5796.

29. Wu FH, Chai TY. Soft sensing method for magnetic tube recovery ratio via fuzzy systems and neural networks. *Neurocomputing*. 2010;73(13–15):2489-2497.

30. Yu J. A Bayesian inference based two-stage support vector regression framework for soft sensor development in batch bioprocesses. *Comput Chem Eng*. 2012;41(11):134-144.

31. Zhang SN, Wang FL, He DK, Jia R. Real-time product quality control for batch processes based on stacked least-squares support vector regression models. *Comput Chem Eng*. 2012;36(10):217-226.

32. Cheng C, Chiu MS. A new data-based methodology for nonlinear process modeling. *Chem Eng Sci*. 2004;59(13):2801-2810.

33. Fujiwara K, Kano M, Hasebe S, Takinami A. Soft-sensor development using correlation-based just-in-time modeling. *AIChE J*. 2009;55(7):1754-1765.

34. Yuan X, Ge Z, Huang B, et al. A probabilistic just-in-time learning framework for soft sensor development with missing data. *IEEE Trans Control Syst Technol*. 2016;25(3):1-9.

35. Shao W, Tian X, Wang P. Soft sensor development for nonlinear and time-varying processes based on supervised ensemble learning with improved process state partition. *Asia-Pac J Chem Eng*. 2015;10(2):282-296.

36. Gopakumar V, Tiwari S, Rahman I. A deep learning based data driven soft sensor for bioprocesses. *Biochem Eng J*. 2018;136:28-39.

37. Yan W, Tang D, Lin Y. A data-driven soft sensor modeling method based on deep learning and its application. *IEEE T Ind Electron*. 2017;64(5):4237-4245.

38. Yuan X, Ou C, Wang Y, Yang C, Gui W. Deep quality-related feature extraction for soft sensing modeling: a deep learning approach with hybrid VW-SAE. *Neurocomputing*. 2019. https://doi.org/10.1016/j.neucom.2018.11.107

39. Yuan X, Zhou J, Huang B, Wang Y, Yang C, Gui W. Hierarchical quality-relevant feature representation for soft sensor modeling: a novel deep learning strategy. *IEEE. T. Ind. Inform.*, 2019. https://doi.org/10.1109/TII.2019.2938890

40. Wang Y, Pan Z, Yuan X, Yang C, Gui W. A novel deep learning based fault diagnosis approach for chemical process with extended deep belief network. *ISA. T.*, 2019. https://doi.org/10.1016/j.isatra.2019.07.001

41. Zuo X, Tu F, Qing HY, et al. Advanced control of acetylene hydrogenation reactor (II). Soft sensor and its engineering practice. *Control Instr Chem Ind (China)*. 2003;30(2):19-21.

42. Yuan X, Wang Y, Yang C, Ge Z, Song Z, Gui W. Weighted linear dynamic system for feature representation and soft sensor application in nonlinear dynamic industrial processes. *IEEE T Ind Electron*. 2018;65(2):1508-1517.

43. Yuan X, Li L, Wang Y. Nonlinear dynamic soft sensor modeling with supervised long short-term memory network. *IEEE. T. Ind. Inform.*, 2019. https://doi.org/10.1109/TII.2019.2902129

44. Hu J, Wang Z, Gao H, Stergioulas L. Extended Kalman filtering with stochastic nonlinearities and multiple missing measurements. *Automatica*. 2012;48(9):2007-2015.

45. Park J, Ahn C, Shi P, Lim M. Self-recovering extended Kalman filtering algorithm based on model-based diagnosis and resetting using an assisting FIR filter. *Neurocomputing*. 2016;173:645-658.

46. Jiang K, Geng P, Meng F, Zhang H. An extended Kalman filter for input estimations in diesel-engine selective catalytic reduction applications. *Neurocomputing*. 2016;171:569-575.

47. Einicke G, White L. Robust extended Kalman filtering. *IEEE Trans Signal Process*. 1999;47(9):2596-2599.

48. Xiong K, Wei C, Liu L. Robust extended Kalman filtering for nonlinear systems with stochastic uncertainties. *IEEE Trans Syst Man Cybern PartA:Syst Hum*. 2010;40(2):399-405.

49. Kulikov GY, Kulikova MV. Accurate numerical implementation of the continuous-discrete extended Kalman filter. *IEEE T Automat Contr*. 2014;59(1):273-279.

50. Kulikov GY, Kulikova MV. High-order accurate continuous-discrete extended Kalman filter for chemical engineering. *Eur J Control*. 2015;21:14-26.

51. Kulikov GY, Kulikova MV. The accurate continuous-discrete extended Kalman filter for radar tracking. *IEEE T Signal Proces*. 2016;64(4):948-958.

52. Xie FM, Xu F, Liang ZS, Luo XL, Shi ZY. Full-cycle operation optimization of acetylene hydrogenation reactor. *CIESC J*. 2018;69(3):1081-1091.

53. Sinopoli B, Schenato L, Franceschetti M, Poolla K, Jordan MI, Sastry SS. Kalman filtering with intermittent observations. *IEEE T Automat Contr*. 2018;69(3):1081-1091.

54. Julier SJ, Uhlmann JK. Unscented filtering and nonlinear estimation. *Proc IEEE*. 2004;92(3):401-422.